



## **The role of fine excipient particles in adhesive mixtures for inhalation**


Downloaded from: <https://research.chalmers.se>, 2025-12-04 20:03 UTC

Citation for the original published paper (version of record):

Tamadondar, M., Salehi, K., Abrahamsson, P. et al (2021). The role of fine excipient particles in adhesive mixtures for inhalation. AICHE Journal, 67(5). <http://dx.doi.org/10.1002/aic.17150>

N.B. When citing this work, cite the original published paper.

# The role of fine excipient particles in adhesive mixtures for inhalation

Mohammad R. Tamadondar<sup>1</sup> | Kian Salehi<sup>1</sup> | Per Abrahamsson<sup>2</sup> |  
Anders Rasmuson<sup>1</sup> 

<sup>1</sup>Department of Chemistry and Chemical Engineering, Chalmers University of Technology, Gothenburg, Sweden

<sup>2</sup>Technical Analysis, Fluid Mechanics, AFRY, Gothenburg, Sweden

## Correspondence

Anders Rasmuson, Department of Chemistry and Chemical Engineering, Chalmers University of Technology, Gothenburg, Sweden.

Email: rasmuson@chalmers.se

## Funding information

Vetenskapsrådet, Grant/Award Number: 621-2014-4196

## Abstract

Despite the fact that adding fines improve the drug dispersion performance during inhalation, the scarcity of mechanistic insight into the formulation process, independent of the aerosolization, has kept the dispute on the underlying improvement mechanism open. We therefore simulate ternary formulations (carrier, drug, fines) in a vibrational cell to explore the mixing mechanism and the effect of particle size and loading ratio of fines on formulation performance. Results suggest that the buffer theory is a critical contributory mechanism since it curtails the carrier's collision rate and, therefore, decreases agglomerate breakage. Consequently, relatively larger drug aggregates are formed over the carrier, which eventually experiences greater detachment forces. A simple dispersion test is performed to evaluate drug detachment rate at wall-collision. An excess of cohesive fines, or using larger fines, diminishes the rotational kinetic energy of coarse particles by lumping them together. This reduces drug agglomerate breakage and leads to poor mixing.

## KEYWORDS

adhesive mixing, agglomerate breakage, discrete element method, fine excipient particles, ternary formulation

## 1 | INTRODUCTION

The performance of carrier-based dry powder inhalers (DPIs) can be significantly enhanced by the inclusion of a small amount of fine excipient particles into the binary blend of carrier and active pharmaceutical drug particles. *In vitro* measurement of the fine particle dose (FPD) or the fine particle fraction (FPF) of drug particles that is delivered by the inhaler is normally used as a major indicator of this enhancement. Extensive research on the carrier-fine-drug ternary mixture have shown that fine excipient particles improve the performance of DPI formulation to varying extents depending on the excipient's material, the amount and size of the fine particles, and the

blending sequence of mixture components. A comprehensive review article compiled by Jones and Price<sup>1</sup> contains detailed information on the examined DPI formulations and the influence of additional fine particles on FPD and FPF.

An unsettled question on the contribution of fine excipient particles in the DPI formulation is the underlying mechanisms by which the performance of carrier-based ternary mixture increases. Initially, two main theories have been proposed in the literature to address this question (see Figure 1):

- a. *The active site theory* suggests that carrier surface activity has a heterogeneous distribution, and fine excipient particles compete

This is an open access article under the terms of the Creative Commons Attribution-NonCommercial-NoDerivs License, which permits use and distribution in any medium, provided the original work is properly cited, the use is non-commercial and no modifications or adaptations are made.

© 2021 The Authors. *AIChE Journal* published by Wiley Periodicals LLC. on behalf of American Institute of Chemical Engineers.

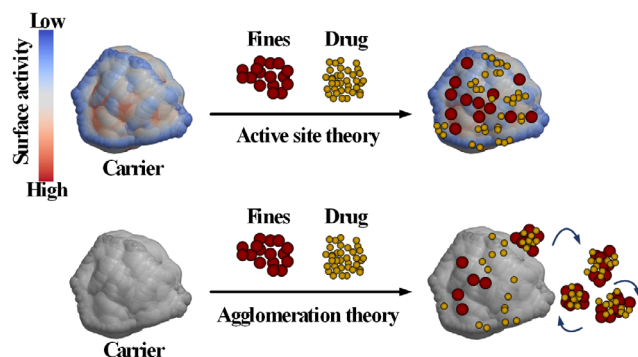


**FIGURE 1** The hypothetical mechanisms by which fine excipient particles improve DPI formulation performance. The active site theory suggests the occupation of the carriers' strongest binding sites by fine excipient particles, and the agglomeration theory supports the idea of the formation of fine-drug agglomerates during blend preparation [Color figure can be viewed at [wileyonlinelibrary.com](http://wileyonlinelibrary.com)]

with drug particles for high-energy binding sites. This competition forces the drug particles to interact with passive or low energy sites, which facilitates drug-carrier detachment.<sup>2-4</sup>

- b. *The agglomeration theory* focuses on the possible formation of fines-drug aggregates during blending. These agglomerates are subject to stronger aerodynamic drag forces during aerosolization than small drug particles, which results in a higher FPD.<sup>5-7</sup>

Supporting evidence of the active site theory was extracted by studying the effect of the blending order of mixture components on formulation performance. Related research has demonstrated that the fine particle delivery of a formulation prepared, first, by blending carrier and fines and then adding the drug is greater than a formulation prepared by adding fines after blending carrier and drug particles. It has been proposed that, in the first mixing scenario, fines have the advantage of establishing contact with more adhesive sites, while in the second scenario, the strong binding sites of the carrier are occupied by drug particles instead. As the powder is subjected to aerosolization, the first mixture releases more drug particles than the second mixture due to the relative strength of carrier-drug binding forces. A study by Zeng et al<sup>8</sup> has illustrated that, by mixing the components long enough (from 15 to 60 min), the blending sequence becomes insignificant, indicating that fines and drug particles continue to redistribute until they reach an equilibrium state over the carrier surface.

The active site theory has been found unsatisfactory, or even contradictory, in explaining the results of some in vitro performance tests of ternary carrier-based DPI formulations.<sup>1</sup> For instance, Jones et al<sup>9</sup> have shown, using direct measurement of adhesion and cohesion forces between particles, that contrary to the prediction of active site theory, a more adhesive fine particle does not ensure a larger FPD. Such experimental observations relate the improvement in DPI performance to the theory of fines-drug agglomeration. This theory hypothesizes that once the drug particles have been contained in agglomerated structures with larger mass, they experience greater

aerodynamic forces and, consequently, liberate easier from the carrier surface. The agglomeration theory also clarifies additional ambiguities, including the behavior of FPF with a critical ratio of drug/fine in ternary DPI formulation. Islam et al<sup>10</sup> have observed that if this ratio goes beyond one, the excess of drug particles leads to the formation of so-called drug multiplets with strong adhesive interactions that eventually decrease the FPF.

Besides these two major theories, additional mechanisms have been proposed and supported with empirical evidence to explain the effect of added fines. One is the so-called *fluidization reinforcement hypothesis*,<sup>11</sup> which argues that the presence of fines increases the tensile strength of the powder bulk, and thereby, shifts the minimum fluidization velocity (MFV) in the inhalation chamber. This phenomenon intensifies interparticle collisions and enhances the likelihood of drug-carrier de-agglomeration. Dickhoff et al<sup>12</sup> have introduced the *buffer hypothesis*, which states that fines act as a buffer between colliding carriers and protect drug particles from press-on forces. According to this theory, the fine particles aid dispersion only if the fine/drug particle size ratio is above one, as the sheltering effect depends on this size disparity. The idea that fines promote the disintegration of cohesive drug agglomerates has been also proposed and discussed by Shalash and Elsayed.<sup>13</sup>

While these mechanisms appear plausible, they remain as speculations due to the abundance of experimental findings under similar conditions that support alternative choices. One shortcoming that leads to such discrepancies in the assessment of DPI performance is the lack of a mechanistic understanding of ternary mixing, and therefore, it is crucial to investigate formulation performance independent of the aerosolization process (i.e., FPD or FPF). To address this issue, we performed a numerical simulation of adhesive binary and ternary mixing in a high-intensity vibrational cell, wherein the primary objective was to unravel the effect of added fines on the quality of mixture. The Discrete Element Method (DEM) was used for the simulation of particle movement to gain fine temporal and spatial resolutions on the particles. Complex-shaped carriers were mathematically described using Fourier harmonics,<sup>14</sup> which is a novel method to incorporate irregularity and roughness into a particle's morphology. This method also allows a non-uniform distribution to be imposed onto carrier surface activity. The adhesive mixing process was explored through analysis of drug and fine agglomerate breakage, particle contact numbers, and interparticle adhesion forces.

## 2 | THEORETICAL CONSIDERATIONS

### 2.1 | Rough particles in contact

The contact area between two particles is a fundamental factor in determining adhesion force, and surface asperities can drastically change this factor. Experimental observations have revealed that the real contact area for particle interaction is less than 15% of the apparent contact area that is estimated from particle size and physical properties.<sup>15</sup> Since particle surfaces are nominally flat, a proper contact

model must account for particle roughness. The Greenwood and Williamson (GW) model is one of the classical approaches for incorporating surface roughness into the contact mechanism.<sup>16</sup> In this approach, a Gaussian distribution of  $\varphi(z)$  for the asperity height is assumed, and the probability of contact is expressed as:

$$\text{prob}(z > d) = \int_d^{\infty} \varphi(z) dz \quad (1)$$

where  $d$  is the separation distance between the reference planes of two contiguous surfaces (Figure 2). In combination with the Hertzian elastic contact theory,<sup>17</sup> the GW model results in a solution to the contact problem of rough surfaces. Moreover, the GW model considers the summit of each asperity as a sphere with a constant curvature that deforms separately under compressive load.

An alternative to the GW model, and other indirect solutions to rough surfaces in the contact (e.g., the fractal model by Majumder and Bhushan<sup>18</sup>), is to approximate the microscale nature of a rough surface and explicitly resolve the contact model for each individual asperity on that surface (Figure 2). The latter method suggests that the magnitude of contact force depends on the radius of curvature at the contact point corresponding to each asperity height. This approach relies, first, on the mathematical definition of surface roughness and, second, on the method to make this definition compatible with the simulation environment.

## 2.2 | Particle adhesion force distribution

The morphological variations in the contact zone of contiguous surfaces imply a distribution of adhesion force on rough surfaces. Three types of distributions have been identified with a direct measurement of adhesion force using the atomic force microscopy (AFM) technique<sup>19</sup>:

- Type I: Weibull distribution, which applies to the adhesion of relatively smooth particles to substrates with a narrow distribution of the asperity radius.
- Type II: bimodal Weibull distribution, which describes the adhesion between particles and substrates with similar orders of magnitude of roughness.

- Type III: log-normal distribution, which corresponds to surfaces with rather broad heterogeneity in asperity size distributions.

AFM measurements at multiple sites on the surface of different lactose particle samples have shown that the adhesion force exhibits Type III, that is, log-normal, distribution, and this can be expressed by the geometric mean force and the geometric standard deviation.<sup>20,21</sup> An example of AFM data for a Pharmatose 325 M particle is shown in Figure 3.<sup>20</sup> Results of these measurements also fit the definition of carrier surface activity by Grasmeijer et al.,<sup>22</sup> wherein the carrier particle has a range of surface-free energy and promises different abilities in retaining drug particles during dispersion. This innate nonuniformity of adhesion force is an essential element of the ternary DPI formulation, and therefore, the simulation framework must allow for such a characteristic.

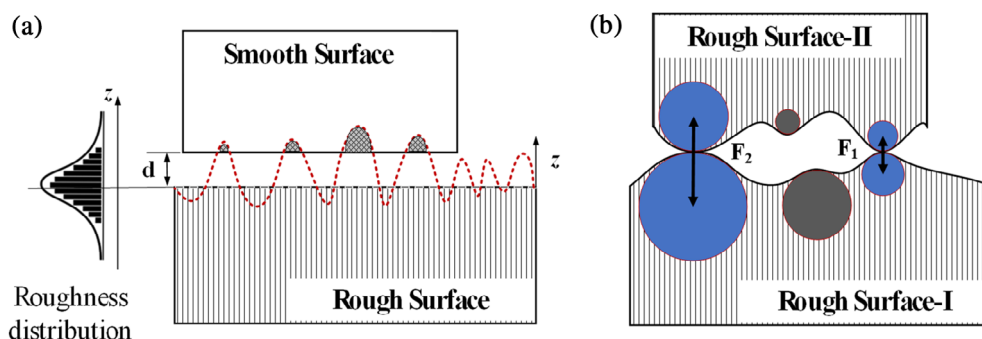
## 2.3 | Computational framework

The classical soft-sphere discrete element method was used to perform the simulation of a particulate system. The contact mechanism between colliding particles is the core of the DEM integration scheme and is normally expressed in the form of contact force versus overlap. This relationship depends on the material properties of the particles, the sizes of the two particles in contact, and their surface conditions. Contact force and, consequently, contact torque are used to update the translational and rotational velocities of particles. The intrinsic dominance of adhesion between micron-sized particles entails using an adhesive contact model. Two models, the Johnson-Kendall-Roberts (JKR) theory<sup>23</sup> and the Derjaguin-Muller-Toporov (DMT) theory<sup>24</sup> are common to use in DEM codes. These two models represent opposite extremes, as described by Maugis,<sup>25</sup> and the transition between them can be predicted from the dimensionless parameter of  $\lambda$  defined as:

$$\lambda = \frac{2.06}{z_0} \sqrt[3]{\frac{\Gamma_{ij}^2 R^*}{\pi E^* z^2}} \quad (2)$$

JKR applies if  $\lambda > 5$  and DMT applies if  $\lambda < 0.1$ . This criterion is recommended over the Tabor number, as the latter one is argued to sometimes lead to a poor choice of adhesive model.<sup>26</sup> Among all the possible contacts in the present simulation environment, the  $\lambda$  number

**FIGURE 2** (A) Theoretical scheme of the Greenwood-Williamson model of a rough surface in contact with a smooth surface, and (B) approximating the microscale nature of the rough surfaces with spherical elements in order to explicitly resolve the contact problem [Color figure can be viewed at [wileyonlinelibrary.com](http://wileyonlinelibrary.com)]



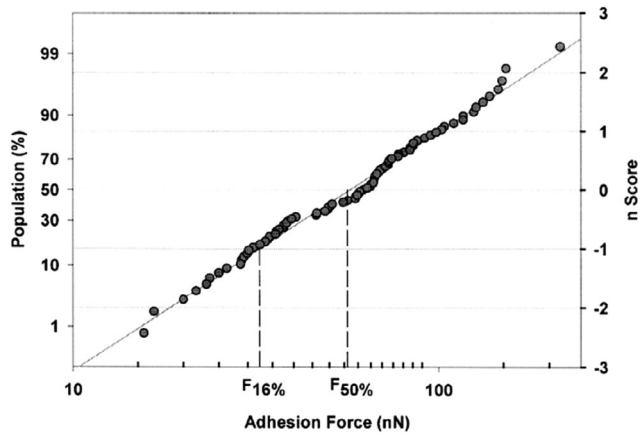


**FIGURE 3** The adhesion force distribution of 325 M lactose particles shows that the data follows a log-normal distribution, with a regression coefficient of 0.99 (Louey et al. <sup>7</sup>).  
Source: Reprinted with permission from Elsevier

is the least (around 4) for drug–drug contacts because of the smallest contact radius and largest effective Young modulus. Based on the Maugis dimensionless number, the elastic JKR model was chosen as an apt model for calculating the contact force in the subsequent simulations of this study. Moreover, the validity of the JKR theory in modeling the adhesive behavior of particles, especially in the context of pharmaceutical powders used in the inhalation process, is well established.<sup>27–29</sup>

In the JKR model, the contact is considered to be adhesive over a finite area, which is correlated to elastic material properties and particles surface energy. The dependency of contact area radius ( $a$ ) to normal force ( $F_{ne}$ ) is given as:

$$a^3 = \frac{3R^*}{4E^*} \left( F_{ne} + 3\pi\Gamma_{ij}R^* \pm \sqrt{6\pi\Gamma_{ij}R^*F_{ne} + (3\pi\Gamma_{ij}R^*)^2} \right) \quad (3)$$

where only the positive root is allowed for stable equilibrium. According to the force–contact area relationship of the JKR interaction, in the loading regime and comparing to the common Hertzian contact model,<sup>17</sup> Equation (3) will generate a larger contact area due to attractive interaction. As a result of this attraction, a finite contact area occurs even under zero external load (equilibrium contact area) and its radius is equal to:

$$a_0^3 = \frac{9\Gamma_{ij}\pi R^{*2}}{2E^*} \quad (4)$$

According to this theory, the maximum tensile force required to break a contact depends on the effective radius of curvature and the surface energy of the particles in contact.

$$F_C = \frac{3}{2}\pi\Gamma_{ij}R^* \quad (5)$$

This expression is commonly used to describe the magnitude of the pull-off force measurement in the AFM experiment. The corresponding particle overlap at the critical point is defined as:

$$\delta_C = \frac{a_0^2}{2(6)^{\frac{1}{3}}R^*} \quad (6)$$

From a computational point of view, having critical force and overlap as well as normal overlap can lead to the calculation of contact radius and, eventually, the normal elastic force. The procedure for this calculation is based on the following expressions:

$$\frac{\delta_n}{\delta_C} = 6^{\frac{1}{3}} \left[ 2 \left( \frac{a}{a_0} \right)^2 - \frac{4}{3} \left( \frac{a}{a_0} \right)^{\frac{3}{2}} \right] \quad (7)$$

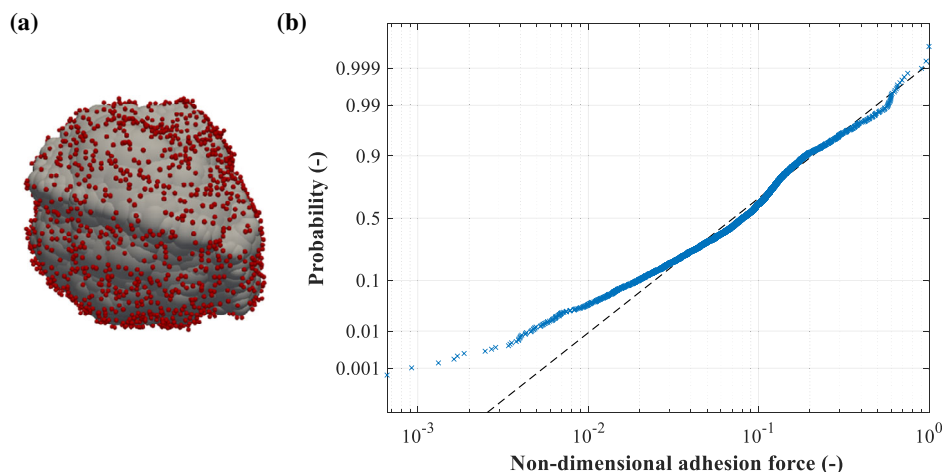
$$\frac{F_{ne}}{F_C} = \left[ 4 \left( \frac{a}{a_0} \right)^3 - 4 \left( \frac{a}{a_0} \right)^{\frac{3}{2}} \right] \quad (8)$$

## 2.4 | Generating realistic particles for DEM

While the conventional DEM framework conceives of particles as smooth spherical elements, such ideal morphological features are a rarity in the common carrier particles used in DPI formulations. Therefore, a non-spherical scheme must be applied for the simulation of an adhesive ternary system to account for the shape irregularity and surface roughness of particles. To meet this requirement, the multisphere model, introduced by Favier et al.,<sup>30</sup> was selected for creating complex-shaped particles. In this model, the particle is represented by overlapping spheres, fixed rigidly with respect to a local coordinate system. Since contact detection remains sphere-based, this model offers the least complexity in defining a contact plane, particle overlap, and frictional forces.

A prior step to creating a particle with a multisphere model is to define the shape outline. In this study, the Fourier-based method for creating realistic granular samples developed by Mollon and Zhao<sup>31</sup> was used. Initially, the original shape of a particle is quantified using the closed-form Fourier series to obtain the spectrum of Fourier shape descriptors.<sup>32</sup> This mathematical definition leads to a series of spatial points that describe the particle outline, and ultimately, a tessellated surface of particle convex-hull is generated. Once the particle outline has been generated, it is replaced with an equivalent collection of overlapping spheres for future DEM simulation. The mathematical algorithm to achieve a multisphere model from the 3D convex-hull is commonly known as an Overlapping Discrete Element Cluster (ODEC). The 3D ODEC algorithm proposed by Ferrellec and McDowell<sup>33</sup> was selected as the basis of the present study. In this algorithm, an arbitrary point is chosen on the surface of convex-hull, then a sphere is grown along its internal normal direction and is expanded until it reaches another point on the surface of the particle. This procedure continues until there is one sphere for each point. The accuracy of the shape approximation of the multisphere model is improved by increasing the resolution of surface discretization as well as introducing more spheres, each with a small radius. Complex-shaped

**FIGURE 4** (A) The carrier particle is coated with 2000  $\mu\text{m}$ -sized adhesive particles to calculate contact force and extract surface activity. (B) Distribution of the non-dimensional adhesion force of the selected carrier [Color figure can be viewed at [wileyonlinelibrary.com](http://wileyonlinelibrary.com)]



particles have been created with this method in earlier works by the authors, wherein the effect of the target particle shape on the breakage and adhesion pattern of a colliding agglomerate was investigated.<sup>34</sup>

### 3 | SIMULATION SETUP

#### 3.1 | Coarse particle

An integral feature of DEM with a multisphere model is that it allows the local contact properties of a single particle to be manipulated, including the radius of curvature. This feature allows the creation of a particle with a targeted distribution of surface adhesion force, for example, log-normal distribution. For this purpose, a series of Fourier shape descriptors are obtained from real particle shapes, and their corresponding coarse carrier particles are generated in the simulation domain. Once the carrier particle has been generated, the adhesion force distribution can be extracted based on the following steps:

1. A virtual spherical domain is created around the carrier particle, wherein 2000 adhesive micronized particles are randomly inserted.
2. The adhesive particles are gradually dragged toward the carrier surface by minute-scale impetus force until the contact is stabilizes and the kinetic energy of the particles entirely dissipates.
3. The magnitude of the adhesion force between the carrier and small particles is obtained and turned into a dimensionless quantity by using the corresponding minimum and maximum values. In this way, the non-dimensional adhesion force distribution becomes a unique feature of a coarse carrier particle.

The distribution of the dimensionless adhesion force was examined, and the carrier with the closest fit to the log-normal distribution was selected for the purpose of this study. Figure 4 shows the selected carrier with 2000 adhesive particles of 2  $\mu\text{m}$  diameter deposited over its surface as well as the corresponding distribution of non-dimensional adhesion force. One can discern a deviation from log-normal on the left side of the distribution plot, which corresponds to

**TABLE 1** Physical properties of the particles and other simulation settings

Particle properties	Carrier	Fine	Drug
Particle size ( $\mu\text{m}$ )	80 <sup>a</sup>	5 <sup>b</sup>	3
Number of particles	3	700 <sup>b</sup>	900
Particle density <sup>36,37</sup> ( $\text{kg}/\text{m}^3$ )	1,550	1,550	1,330
Young modulus <sup>38</sup> (GPa)	0.1	0.1	2
Poisson ratio <sup>39</sup> (—)	0.29	0.29	0.3
Surface energy <sup>27</sup> ( $\text{J}/\text{m}^2$ )	0.005	0.008	0.015
Friction coefficient <sup>40,41</sup> (—)	0.3	0.5	0.26
Rolling friction coefficient <sup>42</sup> (—)	0.002	0.002	0.002
<b>Simulation settings</b>			
Time step (s)	$4 \times 10^{-9}$		
Process time (s)	0.5		
Vibration frequency (Hz)	120		
Vibration amplitude ( $\mu\text{m}$ )	200		
Box size ( $\mu\text{m}$ )	$180 \times 180 \times 180$		

<sup>a</sup>The average volumetric size is reported here.

<sup>b</sup>These numbers correspond to the basic ternary formulation.

low values of adhesion force, or equivalently, the small spherical elements that assemble the carrier particle. While this deviation suggests that the small spheres must be excluded for a better fit, the adequacy of shape approximation is dependent on these elements. Therefore, despite the observed deviation, the simulations were conducted with this carrier, as it maintained a balance between distribution fitness and shape approximation adequacy. These simulations were carried out in LIGGGHTS, open-source DEM particle simulation software.<sup>35</sup> The material properties of the carrier were selected based on the lactose particles commonly used in DPI formulation and are presented in Table 1.

#### 3.2 | Drug particle

Since the natural cohesion of drug particles causes them to aggregate, it is essential to introduce these particles in the correct initial



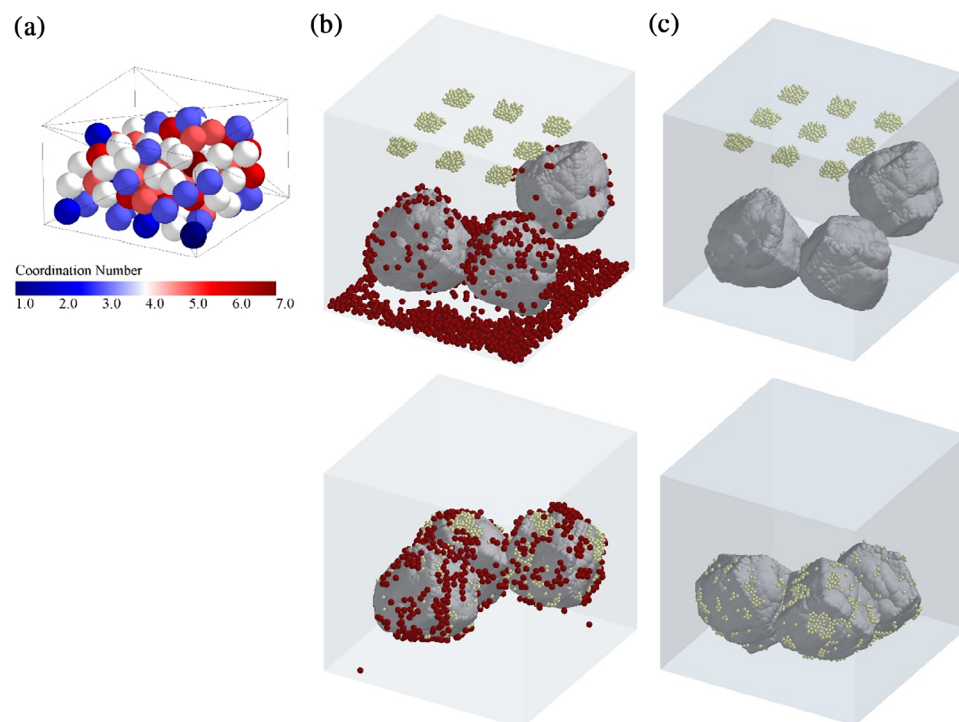


**FIGURE 5** (A) Initial state of a drug agglomerate made of 100 primary particles. (B) A snapshot of particles before and after ternary mixing. (C) A snapshot of particles before and after binary mixing [Color figure can be viewed at [wileyonlinelibrary.com](http://wileyonlinelibrary.com)]

state into the simulation domain. In order to mimic drug agglomeration, the primary particles were randomly generated in a small confined space and settled under gravitational force until they establish cohesive contact, and a stable agglomerate has been formed (i.e., particle kinetic energy has been dissipated). Figure 5A shows an example of the drug agglomerate with 100 constituent particles colored by their coordination number. Mono-sized salbutamol sulfate (SS), as the most frequently investigated drug particle in DPI formulation, was used to resemble the active pharmaceutical particle in the current simulations. The surface energy of drug particle was extracted using Equation (5) and the available AFM data on the pull-off force between SS-probe and SS-substrate.<sup>27</sup> A total of 900 drug particles, equal to a 1.32% w/w mass loading ratio, were added to the formulation. The average volumetric size of a drug agglomerate and its packing fraction were initially 20  $\mu\text{m}$  and 35%, respectively.

### 3.3 | Fine particle

The third component in a simulation of the adhesive mixing process is fine excipient particles. Jones and Price<sup>1</sup> have reported that the conventional practice in the preparation of ternary DPI formulation is to add fine lactose particles with a volume median diameter of (4–7)  $\mu\text{m}$  and proportion in the range of 1.5%–10%. For the current simulations, 700 spherical lactose particles with a diameter of 5  $\mu\text{m}$  (equivalent to the loading ratio of 5.7% w/w) were included in the system. Because excipient particles are heavier and less cohesive than drug particles, the fine particles were introduced individually, that is, in non-agglomerated form. However, since these particles have a natural tendency to cluster, they stuck together after being generated in the

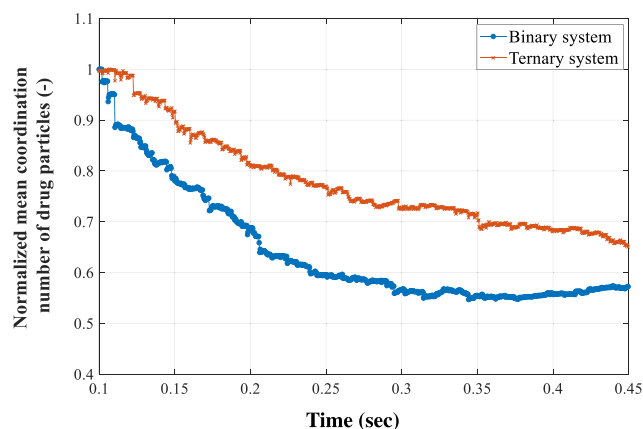


**FIGURE 6** Temporal decay in the average coordinate number of drug particles for ternary and binary systems. The coordination number is normalized after dividing by the maximum value (corresponding to intact agglomerates) [Color figure can be viewed at [wileyonlinelibrary.com](http://wileyonlinelibrary.com)]

simulation environment. The physical and mechanical properties of fine lactose particles are shown in Table 1.

It is important to mention that in the absence of in-house measurement of material properties, literature data were used to obtain particles properties. It is acknowledged that finding the correct material properties for pharmaceutical particles can be an arduous task. These data are sometimes reported to fall within a wide range of values (e.g., the Young modulus of lactose particles) or are rare to find (e.g., the rolling friction coefficient for salbutamol sulfate). In such cases, the corresponding values were adopted from calibrated simulation works.

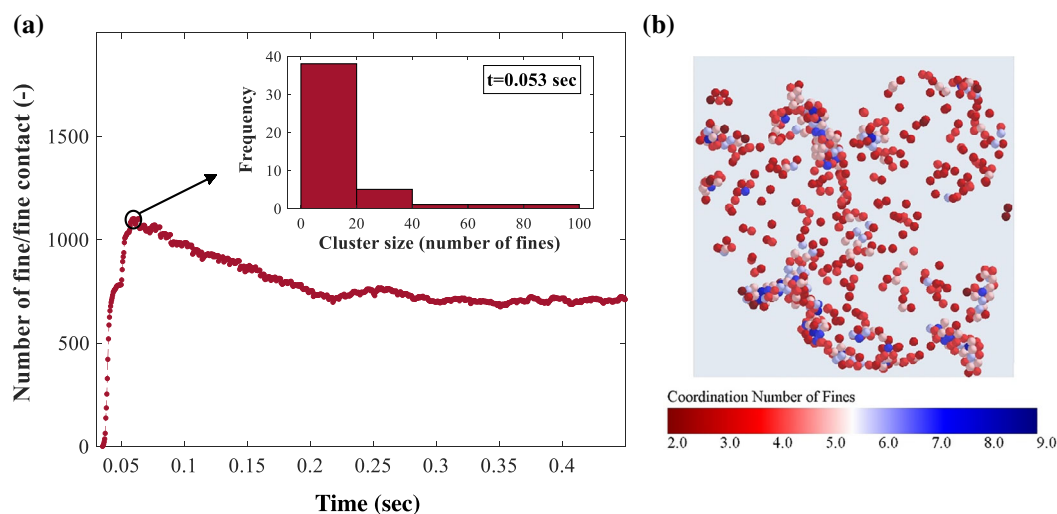


**FIGURE 7** (A) Variation of total contact number for fine particles. The inner graph shows the size distribution of fines clusters at  $t = 0.053$  s, wherein the cluster size is expressed in terms of number of primary particles. (B) Fine particles are colored by coordination number at  $t = 0.053$  s, where the contact number is the largest (the single fines are excluded) [Color figure can be viewed at [wileyonlinelibrary.com](http://wileyonlinelibrary.com)]

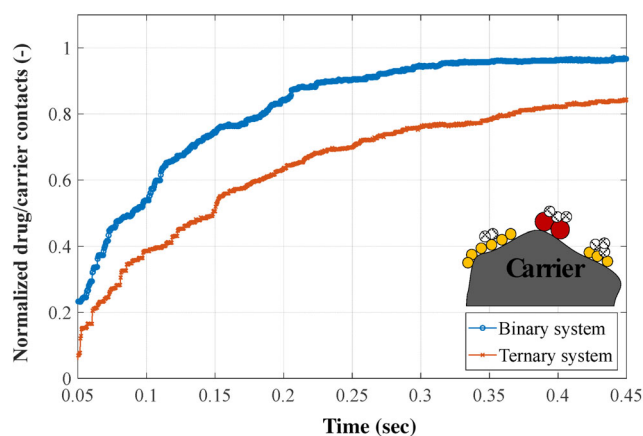


**FIGURE 8** Temporal deposition of drug particles over carrier particles for binary and ternary systems. The value is normalized by the total number of available drug particles. Only the drug particles with direct contact to the carriers are counted (red: fines, yellow: drug with direct contact, white: drug with indirect contact) [Color figure can be viewed at [wileyonlinelibrary.com](http://wileyonlinelibrary.com)]

### 3.4 | Mixing process

The particles were put into the simulation domain by placing the carriers, the fines, and the agglomerates of drug particles in the mixing cell, respectively (Figure 5(B)). In order to avoid heavy computation, the mixer contains only three carrier particles. While it deems necessary to simulate ternary formulations at much larger scale, increasing the number of carriers changes the simulation time drastically not only because the number of spheres in each carrier increases, but also more drug and fine particles are required to keep the loading ratios constant. Sensitivity analysis revealed that increasing the number of carriers to five does not influence the mixing behavior significantly.

The adhesive mixing process was commenced by inducing high-intensity vibration to the cuboidal vessel that contained the particles.

The container was vibrated at a preset amplitude and frequency along the z, y, and x directions. This three-dimensional vibration ensures that kinetic energy is properly transferred to all the particles, and thus, it accelerates the mixing process. To emphasize how the ternary system is different from the binary system, the adhesive mixing of carrier and drug particles, exclusively, was simulated under similar conditions, and the outcomes were compared (Figure 5(C)). The total process time was 0.5 s, which was adequate for this small system of particles. This adequacy was determined by the pseudo steady-state condition in coordination number and kinetic energy of drug and fine particles (see the Appendix S1). After the simulation was completed, the vibration was stopped, and the particles settled inside the container. The vibrational mixing of carrier and drug particles has been simulated in this manner in previous studies to investigate the adhesive mixing process.<sup>43,44</sup> In the present study, simulations of the mixing process were performed using EDEM commercial software, provided by DEM Solutions Ltd.

## 4 | RESULTS AND DISCUSSION

To unravel the role of fine excipient particles, the evolution of mixing was scrutinized by examining the breakage of agglomerates of fines and drugs, the deposition of particles over coarse carriers, the strength of adhesive forces, and the structure of attached layers. Both binary (without fines) and ternary (with fines) mixtures were analyzed to pinpoint the mechanistic effects of the fine particles.

### 4.1 | Breakage of agglomerates

The rate of drug agglomerate breakage was examined by studying the temporal decay in the average coordination number of these particles. The coordination number was extracted at each time step and was



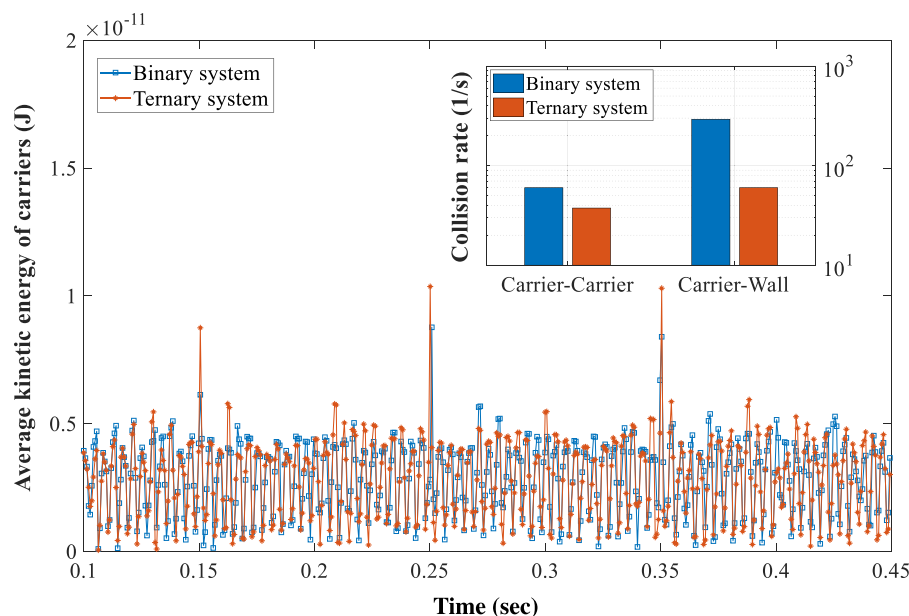


**FIGURE 9** Oscillation of the mean total kinetic energy of carrier particles during mixing in binary and ternary systems. The inner figure shows the differences of carrier-carrier and carrier-wall collision rates between the binary and ternary systems [Color figure can be viewed at [wileyonlinelibrary.com](http://wileyonlinelibrary.com)]

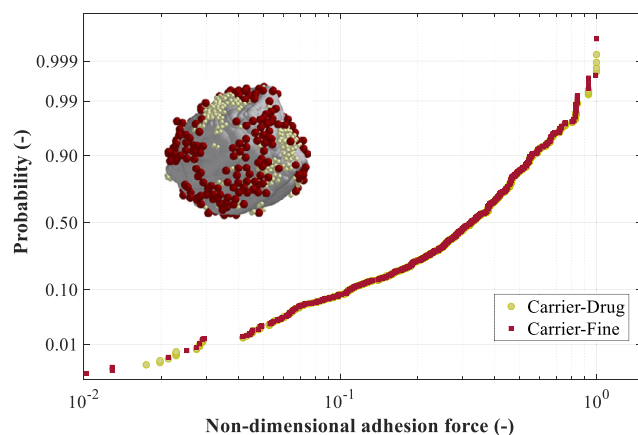


**FIGURE 10** Distribution of adhesive force for carrier-drug and carrier-fine contacts at the completion of ternary mixing. The graph suggests that there is no preference for saturation of carrier active sites by either drug or fine particles [Color figure can be viewed at [wileyonlinelibrary.com](http://wileyonlinelibrary.com)]

normalized by dividing by its maximum value, which was obtained from the initial agglomerate condition. Figure 6 displays the normalized drug coordination number for both binary and ternary mixtures over time and marks the disparity in agglomerate breakage for these two systems. Even though both systems were mixed under similar conditions, the inclusion of fine excipient particles hindered agglomerate breakage.

Besides the rate of drug agglomerate breakage, it is of interest to study the evolution of clusters of fine excipient particles during mixing. Although the primary fine particles were introduced individually into the system, they started to form clusters as contact was established. This phenomenon can be observed by examining the temporal progress of fine-fine contacts at early stages of the mixing, as shown in Figure 7(A). The number of interparticle contacts of fines increased sharply after the vibration started, and it decreased as the

mixing progressed due to the breakage of clusters. Compared to the drug agglomerates, these clusters were weaker, more irregular in shape, and had a broader size distribution (Figure 7(B)). At the peak of the contact number, the mixture contained a few large and free clusters, consisting of 40–100 primary fine particles, while at the completion of mixing, the fine particles were in smaller clusters and attached to the carriers.

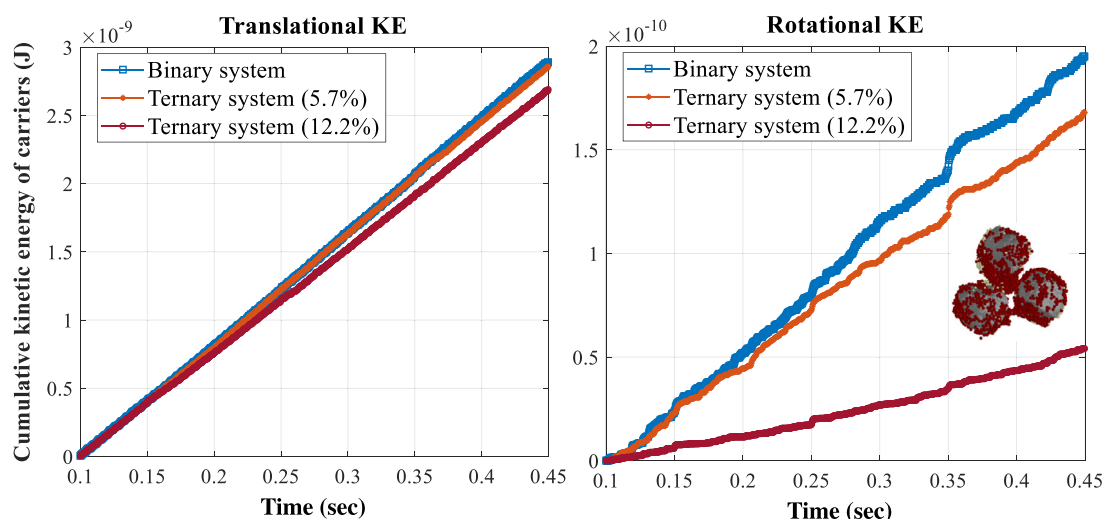
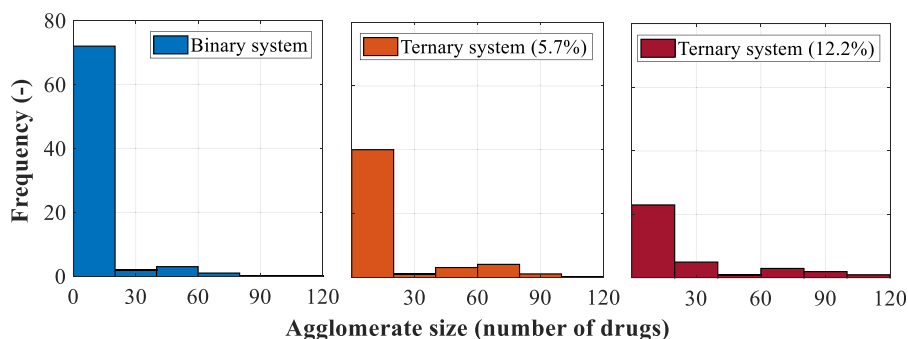
However, a comparatively lower breakage rate for drug agglomerates in a ternary system does not necessarily indicate a poorer degree of mixing for such systems. An assessment of drug particle distribution over the carriers revealed that, in the final state of mixing, all the drug particles had adhered onto the carrier surface, although in different forms. This difference can be attributed to the contrast between forming a monolayer or a multilayer distribution of drugs over carriers, and it was studied by exploring the number of drug particles directly attached to a carrier particle.

Figure 8 shows the number of carrier-drug direct contacts for the binary and ternary systems. Normalization was done after dividing each value by the total number of drug particles (i.e. 900). The difference in the offset of the two graphs, that is, at the beginning of mixing, is associated with the deposition of drug particles over the fines that are attached to the carriers in the ternary system. Once the mixing of the binary mixture was completed, 97% of all drug particles had been spread over the carrier particles. For the ternary system, a lower percentage of drugs (85%) had directly adhered to the carriers. This disparity signifies that, contrary to the binary system, the drug particles in the ternary system are more likely to attach to carriers in the form of small aggregates. This observation suggests a possible advantage of ternary formulation in aerosolization performance, similar to the assumptions behind the agglomeration theory.

A more intriguing matter is the role of fine particles in hindering the breakage of drug agglomerates. DEM results showed that, in the course of mixing, the average kinetic energy of carrier particles was

**TABLE 2** Critical fine particle attributes for each simulation case

Case number	Fine particle size ( $\mu\text{m}$ )	Fine particle loading ratio (%)	Number of fine particles
Ternary I	5	5.7	700
Ternary II	5	12.2	1500
Ternary III	3	5.7	3241
Ternary IV	7	5.7	255

**FIGURE 11** Size distribution of drug agglomerates after 0.45 s of adhesive mixing. As the loading ratio of fines increases, the surviving agglomerates become larger due to inefficient breakage [Color figure can be viewed at wileyonlinelibrary.com]**FIGURE 12** Cumulative kinetic energy (KE) of coarse particles in three systems, decomposed into translational and rotational components. Due to the cohesion of fine particles, the particles assembly is lumped together, and their relative rotation decreases significantly [Color figure can be viewed at wileyonlinelibrary.com]

alike for both systems, however, the rate of particle-particle and particle-wall collision for carriers was significantly lower in the presence of fine particles (Figure 9). Analogous to what the buffer theory suggests, it was observed here that the fines reduced carrier particle collisions and, thus, protected drug particles from impact. Since the agglomerate breakage in adhesive mixing is governed by continuous collision and friction between coarse particles and drugs,<sup>44,45</sup> the buffer effect of fines prevents further disintegration of drug agglomerates.

It is critical to emphasize that the role of fine particles in buffer theory is more subtle than what is described here. A close examination of “fine lactose fines” (FLF) similar in size to the micronized drug,

and “coarse lactose fines” (CLF) twice the size of micronized drug reveals that fine excipient particles act as a buffer that diminishes the impact on drugs if they are larger than a certain size.<sup>46</sup> Therefore, one must be cautious not to draw a general conclusion on the effect of added fine particles without further parameter variations.

## 4.2 | Assessment of active site theory

Once the mixing was completed, the adhesive contact between carrier-drug and carrier-fine was determined in order to identify possible differences in attachment pattern. The adhesion properties,

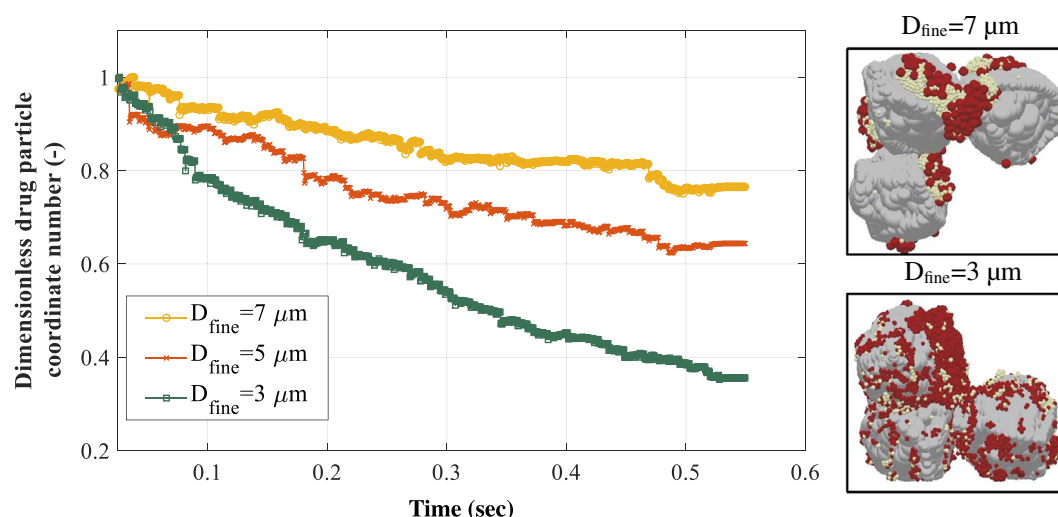


**FIGURE 13** Temporal decay in the average coordinate number of drug particles for ternary systems with different fine particle size. The particle snapshots after 0.5 s of simulation for fine particle sizes of 7 and 3  $\mu\text{m}$  are shown on the right side [Color figure can be viewed at [wileyonlinelibrary.com](http://wileyonlinelibrary.com)]

including the contact force and local contact position for each particle, of the carrier surface were obtained, and the information is displayed in Figure 10 as a comparative probability distribution of adhesion forces. This suggests that, if the active site theory is at work, the carrier sites with lower activity will be covered by drug particles (left tail of the distribution), and the highly active sites of the carrier will be occupied by fine particles (right tail of the distribution). Figure 10 shows the distribution of the average adhesive contact force; the carrier-drug and carrier-fine contacts are distinguished by two colors. It can be seen in the figure that these two distributions are closely matched, implying that the speculative competition between drug and fine particles to adhere onto carriers, as proposed by the active site theory, is not evident in the present simulation. This finding is supported by previous experimental observations that contradict the active site theory: the insignificance of blending order on formulation performance,<sup>5</sup> the ability of drug particles to displace the fines from their carrier binding sites,<sup>7</sup> and the ambiguous effect of carrier particle size on the FPF reported by Islam et al.<sup>47</sup>

#### 4.3 | The effect of fines loading ratio

An intricate aspect of ternary DPI formulation is that the dispersion performance relies on the attributes of the added fine particles, including loading ratio and size. The effect of the first variable is explored by simulating an additional ternary system (case II) with a higher percentage of added fine lactose (12.2% w/w equivalent to 1500 particles, Table 2). Analogous to the behavior at transition from binary to ternary formulation, the breakage of drug agglomerates was further suppressed at a higher loading ratio of fine particles. Comparing the size distribution of drug agglomerates in the three systems, as shown in Figure 11, it can be seen that as more fines are introduced into the system, drug agglomerate breakage slows down, and the surviving agglomerates become larger. This behavior results in poor

mixing because the drug particles do not distribute equally among carrier particles.

While the addition of 5.7% w/w fine particles into the binary system was found to have a negligible effect on the kinetic energy of carrier particles, increasing the mass fraction of fines to 12.2% imposed a noticeable effect on the total kinetic energy. Figure 12 shows the cumulative kinetic energy of carrier particles for three adhesive mixing systems. The translational and rotational components of the kinetic energy are displayed separately. A major change that ensued from the excess of fine particles is the significant decrease in the rotational kinetic energy of coarse particles. This behavior is attributed to the aggregation of coarse particles due to the cohesion of fine particles and the resultant constraint on the dynamic behavior of the carriers. The slow breakage rate for drug agglomerates in the ternary system of 12.2% w/w fines can also be explained in terms of inefficient energy transition to the drug particles due to the collective motion of coarse particles and lack of interparticle collisions.

This phenomenon has been discussed by Shur et al.<sup>11</sup> in the context of the aerosolization process, wherein the cohesion of fines has been observed to increase the tensile strength of the entire powder bed, and therefore, the particles move as a plug. Those authors have argued that this behavior is in favor of the dispersion process because the cohesion of fines shifts the MFV. However, they have not explained how the dispersion enhancement is therapeutically achieved if the expiratory flow rate is obstructed, as is normally the case with patients suffering from chronic respiratory diseases.

#### 4.4 | The effect of fine particle size

There are few experimental works on the role of fine particle size on the performance of DPI ternary formulation. Examination of fine particle size from 3 up to 45  $\mu\text{m}$ <sup>2,48,49</sup> have shown that the greatest FPF of

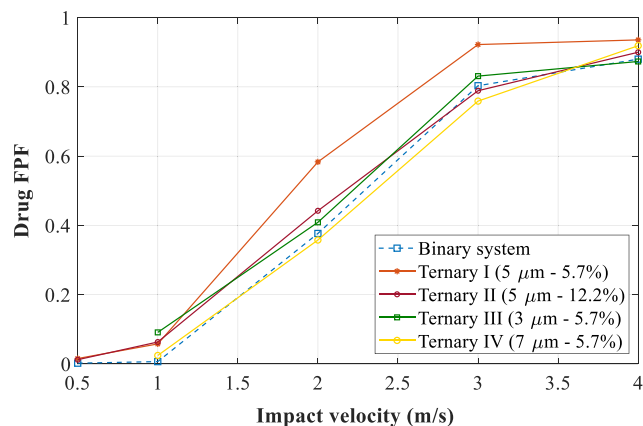


**FIGURE 14** Dispersion of drug particles as a result of wall-collision at different impact velocities [Color figure can be viewed at [wileyonlinelibrary.com](http://wileyonlinelibrary.com)]

drug is achieved when lactose fine particle with the median diameter of  $5.5^{52}$  or  $7.9^{49}$   $\mu\text{m}$  is used. It has been reported that very small fine particles tend to aggregate and progressively occupy the carrier's surface, and very large fine particles act as secondary carriers.

While the influence of fine particles size was briefly discussed in the context of validity of buffer theory, further simulations are required to elucidate the effect of this variable. For this purpose, two supplementary simulations were conducted (cases III and IV in Table 2). These simulations correspond to fine particle sizes of 3 and 7  $\mu\text{m}$  with similar loading ratio of 5.7%.

Evaluation of contact number between mixture components was used to scrutinize the mixing mechanism over time. The behavior of average coordination number of drug particle over time showed that large fine particles hinder the agglomerate breakage significantly (Figure 13). Moreover, the size distribution of drug agglomerates demonstrates that, as the fine particle diameter increases, the size of surviving drug agglomerates increases progressively. This result emphasizes that if the fine particles are large enough, they create a shelter for drug agglomerates against complete disintegration. Besides the sheltering effect, it is crucial to notice that larger fine particles have greater adhesive contact force (Equation 5), which results in constraint on the dynamic behavior of the carriers. The aggregation of coarse particles due to the cohesion of fines was recognized by a significant decline in the rotational kinetic energy of carrier particles in the formulation consisting of large fine particles (similar to Figure 12). Therefore, the size ratio between fine and drug particles is a determinant of ternary formulation performance.

The outcome of these simulations suggested that the extent of drug and carrier particles adhesion is governed by two factors that act in opposite directions. The first one is the number of drug particles in the system, which was found to be inversely correlated to the size of fine particle (more severe agglomerate breakage results in larger number of drug particles). The second factor is the available surface area of the carrier particle for drug particle attachment, which was found to decrease substantially when small fine particles in large number are

present in the system. The simulation results showed that the effect of the first factor outweighs the second one, that is, the overall number of drug-carrier contacts was observed to increase when smaller fine particles were introduced into the ternary formulation.

In addition to imposing an effect on the number of attached drug particles, the fine particle size was observed to change the magnitude of drug-carrier adhesion force. Analysis of variance showed a significant decrease in contact force only for the system with 3  $\mu\text{m}$  fine particle (the size ratio of fine to drug equal to one) with the p-value of 0.005. This behavior is not compatible with the experimental findings of Grasmeyer et al.,<sup>46</sup> primarily because the press-on force has been the controlling adhesion mechanism in their work and this effect was not incorporated into the existing DEM framework.

## 4.5 | Evaluation of drug dispersion

Successive particle-wall collisions are regarded as a contributory mechanism to the detachment of micronized drug particles from carriers in inhalers. In order to evaluate the performance of ternary formulations compared to binary one, the dispersion behavior of each blend was examined according to the following procedure. After the mixing was finalized, the vibrating cell was removed from the simulation domain and the particles assembly, under the influence of gravitational force, were accelerated until they collided with a rigid wall in the normal direction. With this configuration, particle dispersion at five different velocities (corresponding to the average velocity of carrier particles) was tested. The FPF was calculated by obtaining the number of detached drug particles after the collision was completed. Earlier work by the authors<sup>50</sup> has shown that similar wall-impact test of an adhesive unit provides reliable information on the drug dispersion performance in an inhaler. This fact arises from an extremely high rate of wall collision experienced by the carriers and the dominance of particle-wall collision energy over interparticle collisions energy in the dispersion process.<sup>51</sup> In addition, highly resolved CFD-DEM simulation on a single adhesive unit by Cui and Sommerfeld<sup>52</sup> has shown that the probability of the fluid dynamic detachment of micronized particle at the relative velocities that are examined here is quite low, and wall-collision is the controlling mechanism for dispersion.

Figure 14 shows the variation of drug FPF with impact velocity for all the formulations wherein the FPF increases steadily with impact velocity for all cases. Regarding the effect of fine loading ratio, it can be observed that the lowest dispersion efficiency corresponds to the binary formulation. This indicates the improved performance of ternary formulations over binary ones. However, the highest efficiency is observed for the ternary formulation with 5.7% of fine particles, which corroborate the findings that excess of fine particles does not improve the drug dispersion. Concerning the role of fine particle size, the dispersion efficiency is shown to depend on the size of lactose fine particle. The emitted drug particle dose after collision (FPF) is largest when 5  $\mu\text{m}$  fine particle is included in the formulation. It is important to stress that while Figure 14 provides valuable information

regarding the role of formulation variables in a ternary system, these preliminary dispersion results can be subjective to this study and the inherent shortcomings of DEM modeling. Assuredly, a more complex simulation framework for testing the combined effect of flow- and collision-induced dispersion and more elaborate parameter variations are required to attain more conclusive results.

## 5 | CONCLUSION

DEM simulations were used to explore, in microscopic temporal and spatial scales, the role of fines in the context of existing formulation enhancement theories. A vibrating cell that contained a selected set of pharmaceutical particles was used to model the adhesive mixing, and a simple wall-collision test was designed to examine the dispersion performance of adhesive units. The central element of these simulations was to use a complex-shaped carrier particle rather than a single sphere; a feature that led to a surface activity distribution similar to published experimental data.

For our limited set of particle properties, the results showed that fine and drug particles occupy active carrier sites with similar tendencies, and therefore, the active site theory was found implausible. Investigating three different fine particle sizes indicated that larger fine particles hinder the breakage of drug agglomerates more, either by sheltering agglomerates against complete disintegration or by adding to the cohesion of particle assembly and limiting the carriers' motion. These mechanisms result in formation of drug multiplets over the carrier surface. Similar behavior, that is, inefficient drug agglomerate breakage, was observed by increasing the loading ratio of fine particles from 5.7% to 12.2%. The inclusion of cohesive fines added up to the tensile strength of the particle assembly and restricted the rotational motion of coarse particles.

For a deeper insight into the role of fines, the numerical results of a preliminary collision-induced dispersion test were used to evaluate each formulation. Considering all the simplification/assumptions that lay behind our simulations, the FPF values revealed an intriguing result that agreed with existing experimental evidences: the highest dispersion performance was neither attributed to largest fines nor greatest loading ratio, instead an optimal set of system variables are required to achieve the best formulation performance.

Although the current work provides insight into the complexity of adhesive ternary mixing and the influence of some attributes, additional simulations must be carried out based on extensive parameter variations to completely unravel the relevance and limitations of each mechanism. This would mainly include the effect of cohesive-adhesive balance, the particle size distribution of the mixing components, and the mixing intensity in a ternary mixture.

## ACKNOWLEDGMENTS

Financial support from the Swedish Research Council (Grant: 621-2014-4196) is gratefully acknowledged. The authors are thankful for using the code developed by Mollon and Zhao for the purpose of this study, available at: (<http://guilhem.mollon.free.fr/>).

## AUTHOR CONTRIBUTIONS

**Mohammadreza Tamadondar:** Formal analysis; methodology; validation; writing-original draft; writing-review and editing. **Kian Salehi:** Formal analysis; investigation. **Per Abrahamsson:** Formal analysis; investigation. **Anders Rasmuson:** Formal analysis; funding acquisition; investigation; methodology; project administration; resources; supervision; writing-original draft; writing-review and editing.

## DATA AVAILABILITY STATEMENT

Data available on request from the authors.

## ORCID

Anders Rasmuson  <https://orcid.org/0000-0003-0883-052X>

## REFERENCES

1. Jones MD, Price R. The influence of fine excipient particles on the performance of carrier-based dry powder inhalation formulations. *Pharm Res.* 2006;23(8):1665-1674.
2. Zeng XM, Martin GP, Tee S-K, Ghoush AA, Marriott C. Effects of particle size and adding sequence of fine lactose on the deposition of salbutamol sulphate from a dry powder formulation. *Int J Pharm.* 1999; 182(2):133-144.
3. Zeng X, Tee S, Martin G, Marriott C. Improving the delivery efficiency of dry powder inhalers (DPIs) by adding fine carrier particles to powder formulations. *Thorax.* 1996;51(S3):A74.
4. Shah SP, Misra A. Liposomal amikacin dry powder inhaler: effect of fines on in vitro performance. *AAPS PharmSciTech.* 2004;5(4):107-113.
5. Lucas P, Clarke M, Anderson K, Tobyn M, Staniforth J. The role of fine particle excipients in pharmaceutical dry powder aerosols. Paper presented at: Respiratory drug delivery VI; 1998.
6. Lucas P, Anderson K, Staniforth JN. Protein deposition from dry powder inhalers: fine particle multiplets as performance modifiers. *Pharm Res.* 1998;15(4):562-569.
7. Louey MD, Stewart PJ. Particle interactions involved in aerosol dispersion of ternary interactive mixtures. *Pharm Res.* 2002;19(10):1524-1531.
8. Zeng XM, Pandhal KH, Martin GP. The influence of lactose carrier on the content homogeneity and dispersibility of beclomethasone dipropionate from dry powder aerosols. *Int J Pharm.* 2000;197(1-2): 41-52.
9. Jones MD, Hooton JC, Dawson ML, Ferrie AR, Price R. An investigation into the dispersion mechanisms of ternary dry powder inhaler formulations by the quantification of interparticulate forces. *Pharm Res.* 2008;25(2):337-348.
10. Islam N, Stewart P, Larson I, Hartley P. Lactose surface modification by decantation: are drug-fine lactose ratios the key to better dispersion of salmeterol xinafoate from lactose-interactive mixtures? *Pharm Res.* 2004;21(3):492-499.
11. Shur J, Harris H, Jones MD, Kaerger JS, Price R. The role of fines in the modification of the fluidization and dispersion mechanism within dry powder inhaler formulations. *Pharm Res.* 2008;25(7):1631-1640.
12. Dickhoff B, De Boer A, Lambregts D, Frijlink H. The effect of carrier surface treatment on drug particle detachment from crystalline carriers in adhesive mixtures for inhalation. *Int J Pharm.* 2006;327(1-2): 17-25.
13. Shalash AO, Elsayed MM. A new role of fine excipient materials in carrier-based dry powder inhalation mixtures: effect on deagglomeration of drug particles during mixing revealed. *AAPS PharmSciTech.* 2017;18(8):2862-2870.
14. Mollon G, Zhao J. 3D generation of realistic granular samples based on random fields theory and Fourier shape descriptors. *Comput Methods Appl Mech Eng.* 2014;279:46-65.



15. Eve J, Patel N, Luk S, Ebbens S, Roberts C. A study of single drug particle adhesion interactions using atomic force microscopy. *Int J Pharm.* 2002;238(1-2):17-27.
16. Greenwood J, Williamson JP. Contact of nominally flat surfaces. *Proc R Soc Lond Ser A Math Phys Sci.* 1966;295(1442):300-319.
17. Hertz H. Über die Berührung fester elastischer Körper. *J für Die Reine Und Angew Math.* 1882;92:156-171.
18. Majumdar A, Bhushan B. Fractal model of elastic-plastic contact between rough surfaces. *J Tribol.* 1991;113(1):1-11.
19. Göttinger M, Peukert W. Particle adhesion force distributions on rough surfaces. *Langmuir.* 2004;20(13):5298-5303.
20. Louey MD, Mulvaney P, Stewart PJ. Characterisation of adhesional properties of lactose carriers using atomic force microscopy. *J Pharm Biomed Anal.* 2001;25(3-4):559-567.
21. Young PM, Kwok P, Adi H, Chan H-K, Traini D. Lactose composite carriers for respiratory delivery. *Pharm Res.* 2009;26(4):802-810.
22. Grasmeyer F, Frijlink HW, de Boer AH. A proposed definition of the 'activity' of surface sites on lactose carriers for dry powder inhalation. *Eur J Pharm Sci.* 2014;56:102-104.
23. Johnson K, Kendall K, Roberts A. Surface energy and the contact of elastic solids. Paper presented at: proceedings of the Royal Society of London a: mathematical. *Phys Eng Sci.* 1971;324(1558):301-313.
24. Derjaguin BV, Muller VM, Toporov YP. Effect of contact deformations on the adhesion of particles. *J Colloid Interface Sci.* 1975;53(2):314-326.
25. Maugis D. Adhesion of spheres: the JKR-DMT transition using a Dugdale model. *J Colloid Interface Sci.* 1992;150(1):243-269.
26. Drelich J, Tormoen GW, Beach ER. Determination of solid surface tension from particle-substrate pull-off forces measured with the atomic force microscope. *J Colloid Interface Sci.* 2004;280(2):484-497.
27. Begat P, Morton DA, Staniforth JN, Price R. The cohesive-adhesive balances in dry powder inhaler formulations I: direct quantification by atomic force microscopy. *Pharm Res.* 2004;21(9):1591-1597.
28. Hodges CS, Looi L, Cleaver JA, Ghadiri M. Use of the JKR model for calculating adhesion between rough surfaces. *Langmuir.* 2004;20(22):9571-9576.
29. Butt H-J, Cappella B, Kappl M. Force measurements with the atomic force microscope: technique, interpretation and applications. *Surf Sci Rep.* 2005;59(1-6):1-152.
30. Favier J, Abbaspour-Fard M, Kremmer M, Raji A. Shape representation of axi-symmetrical, non-spherical particles in discrete element simulation using multi-element model particles. *Eng Comput.* 1999;16(4):467-480.
31. Mollon G, Zhao J. Fourier-Voronoi-based generation of realistic samples for discrete modelling of granular materials. *Granular Matter.* 2012;14(5):621-638.
32. Ehrlich R, Weinberg B. An exact method for characterization of grain shape. *J Sediment Res.* 1970;40(1):205-212.
33. Ferrellec J-F, McDowell GR. A method to model realistic particle shape and inertia in DEM. *Granular Matter.* 2010;12(5):459-467.
34. Tamadondar MR, de Martin L, RA. Agglomerate breakage and adhesion upon impact with complex-shaped particles. *AIChE J.* 2019;65(6):e16581.
35. Kloss C, Goniva C. LIGGGHTS: a new open source discrete element simulation software. Paper presented at: Proceedings of The Fifth International Conference on Discrete Element Methods, London, UK; 2010.
36. Kaialy W, Martin GP, Larhrib H, Ticehurst MD, Kolosionek E, Nokhodchi A. The influence of physical properties and morphology of crystallised lactose on delivery of salbutamol sulphate from dry powder inhalers. *Colloids Surf B Biointerfaces.* 2012;89:29-39.
37. Chiou H, Li L, Hu T, Chan H-K, Chen J-F, Yun J. Production of salbutamol sulfate for inhalation by high-gravity controlled antisolvent precipitation. *Int J Pharm.* 2007;331(1):93-98.
38. Harris H. *Rapid preformulation screening of drug candidates for dry powder inhaler preparation.* Bath, England: University of Bath; 2008.
39. Boerefijn R, Ning Z, Ghadiri M. Disintegration of weak lactose agglomerates for inhalation applications. *Int J Pharm.* 1998;172(1-2):199-209.
40. Domike RD. *Pharmaceutical powders in experiment and simulation: towards a fundamental understanding.* Massachusetts, USA: Massachusetts Institute of Technology; 2004.
41. Yu S. *Roll compaction of pharmaceutical excipients.* Birmingham, England: University of Birmingham; 2013.
42. Tong Z, Yang R, Yu A, Adi S, Chan H-K. Numerical modelling of the breakage of loose agglomerates of fine particles. *Powder Technol.* 2009;196(2):213-221.
43. Yang J, Wu C-Y, Adams M. DEM analysis of particle adhesion during powder mixing for dry powder inhaler formulation development. *Granular Matter.* 2013;15(4):417-426.
44. Deng X, Zheng K, Davé RN. Discrete element method based analysis of mixing and collision dynamics in adhesive mixing process. *Chem Eng Sci.* 2018;190:220-231.
45. Tamadondar MR, Rasmuson A, Thalberg K, Niklasson Björn I. Numerical modeling of adhesive particle mixing. *AIChE J.* 2017;63(7):2599-2609.
46. Grasmeyer F, Lexmond AJ, van den Noort M, et al. New mechanisms to explain the effects of added lactose fines on the dispersion performance of adhesive mixtures for inhalation. *PLoS One.* 2014;9(1):e87825.
47. Islam N, Stewart P, Larson I, Hartley P. Effect of carrier size on the dispersion of salmeterol xinafoate from interactive mixtures. *J Pharm Sci.* 2004;93(4):1030-1038.
48. Adi H, Larson IC, Stewart PJ. Influence of particle size of the fine lactose in the dispersion of salmeterol xinafoate from lactose mixtures for inhalation. Paper presented at: Biological Pharmaceutical Clinical & Regulatory Issues Related to Optimized Drug Delivery by Aerosol; 2004.
49. Stewart P, Adi H, Larson I. Dry powder inhaler formulations: simple two component powder mixtures or a multi-particulate nightmare. *Drug Deliv Lungs.* 2005;16:81Y84.
50. Tamadondar MR, Rasmuson A. The effect of carrier surface roughness on wall collision-induced detachment of micronized pharmaceutical particles. *AIChE J.* 2020;66(1):e16771.
51. Tong Z, Kamiya H, Yu A, Chan H-K, Yang R. Multi-scale modelling of powder dispersion in a carrier-based inhalation system. *Pharm Res.* 2015;32(6):2086-2096.
52. Cui Y, Sommerfeld M. Forces on micron-sized particles randomly distributed on the surface of larger particles and possibility of detachment. *Int J Multiph Flow.* 2015;72:39-52.

## SUPPORTING INFORMATION

Additional supporting information may be found online in the Supporting Information section at the end of this article.

**How to cite this article:** Tamadondar MR, Salehi K, Abrahamsson P, Rasmuson A. The role of fine excipient particles in adhesive mixtures for inhalation. *AIChE J.* 2021; e17150. <https://doi.org/10.1002/aic.17150>